J. Membrane Biol. 126, 1–18 (1992)

The Journal of
Membrane Biology

Membrane Transport in Stomatal Guard Cells: The Importance of Voltage Control

G. Thiel*, E.A.C. MacRobbie, and M.R. Blatt**
Botany School, University of Cambridge, Cambridge CB2 3EA, England

Summary. Potassium uptake and export in the resting conditions and in response to the phytohormone abscisic acid (ABA) were examined under voltage clamp in guard cells of *Vicia faba* L. In 0.1 mM external K^+ (with 5 mM Ca^{2+}-HEPES, pH 7.4) two distinct transport states could be identified based on the distribution of the free-running membrane voltage (V_M) data in conjunction with the respective *I-V* and *G-V* relations. One state was dominated by passive diffusion (mean $V_M = -143 \pm 4$ mV), the other (mean $V_M = -237 \pm 10$ mV) exhibited an appreciable background of primary H^+ transport activity. In the presence of pump activity the free-running membrane voltage was negative of the respective K^+ equilibrium potential (E_{K^+}), in 3 and 10 mM external K^+. In these cases V_M was also negative of the activation voltage for the inward rectifying K^+ current, thus creating a strong bias for passive K^+ uptake through inward-rectifying K^+ channels. In contrast, when pump activity was absent V_M was situated positive of E_{K^+} and cells revealed a bias for K^+ efflux. Occasionally spontaneous voltage transitions were observed during which cells switched between the two states. Rapid depolarizations were induced in cells with significant pump activity upon adding 10 μM ABA to the medium. These depolarizations activated current through outward-rectifying K^+ channels which was further amplified in ABA by a rise in the ensemble channel conductance. Current-voltage characteristics recorded before and during ABA treatments revealed concerted modulations in current passage through at least four distinct transport processes, results directly comparable to one previous study (Blatt, M.R., 1990, *Planta* **180**:445) carried out with guard cells lacking detectable primary pump activity. Comparative analyses of guard cells in each case are consistent with depolarizations resulting from the activation of an inward-going, as yet unidentified current, rather than an ABA-induced fall in H^+-ATPase output. Also observed in a number of cells was an inward-directed current which activated in ABA over a narrow range of voltages positive of -150 mV; this and additional features of the current suggest that it may reflect the ABA-dependent activation of an anion channel previously characterized in *Vicia* guard cell protoplasts, but rule out its function as the primary mechanism for initial depolarization. The analyses also yield indirect evidence for a rise in cytoplasmic Ca^{2+} activity in ABA, as well as for a K^+ current distinct from the dominant inward- and outward-rectifying K^+ channels, but neither support nor discount a role for Ca^{2+} influx in depolarizing the membrane. A striking similarity was found for the modulation of inward currents either in response to ABA or after spontaneous depolarizations. This renders the possibility of an agonist (i.e., ABA) activated Ca^{2+} current across the plasma membrane as trigger for the voltage transitions unlikely.

Key Words abscisic acid · *Vicia* stomatal guard cell · membrane depolarization · Ca^{2+} · K^+ · H^+-ATPase · voltage clamp · leak current

Introduction

The stomatal pores which regulate water and gas exchange in leaves open and close as a result of changes in the level of potassium salt accumulation in stomatal guard cells. In turn, these changes are the result of modulations of ion fluxes at guard cell membranes. Stomatal opening is associated with net influx of K^+ at the plasmalemma and either influx of chloride or synthesis of malate in the cytoplasm, whereas stomatal closing follows net efflux of K^+ and anions from the guard cells.

Previous work using *I-V* analysis on intact guard cells (with conventional microelectrodes), or on their protoplasts (with patch-clamp techniques), has documented several putative transport systems capable of providing pathways for K^+ and anion flux across the guard cell plasma membrane. These include (i) an inward-rectifying K^+ transporter (Schroeder, Raschke & Neher, 1987; Schroeder, 1988; Blatt, Thiel & Trentham, 1990), (ii) a strongly outward-rectifying K^+ channel (Blatt, 1987b, 1988, 1990; Blatt & Clint, 1989; Clint & Blatt, 1989; Schroeder et al., 1987; Schroeder, 1988; Hosoi, Iino & Shimizaki, 1988), and (iii) an anion channel, which activates positive of about -80 mV, with a maximum activity around -30 to -40 mV (Keller, Hedrich & Raschke, 1989; Hedrich, Busch & Raschke, 1990).

* *Current address:* Pflanzenphysiologisches Institut, Universität Göttingen, Untere Karspüle 2, 3400 Göttingen, FRG.

** *Current address:* Department of Biochemistry and Biological Sciences, University of London, Wye College, Wye, Kent TN25 5AH, England.

Ion channels are passive elements and their activity requires therefore close control in order to coordinate ion fluxes with the physiological requirements for either guard cell swelling or shrinking. In this respect several possible regulation mechanisms have been deduced from the gating characteristics of the guard cell ion channels. Two striking features and possible sites of regulation for the rectifying K^+ currents (inward and outward) are (i) the marked voltage-dependent gating and (ii) the selective sensitivity of the gating to the cytoplasmic Ca^{2+} activity. The inward rectifying K^+ channel is, at submicromolar concentrations of cytoplasmic Ca^{2+} activated at a voltages negative of about -100 mV, independent of the external K^+ concentration (Schroeder, 1988; Schroeder & Hagiwara, 1989; Blatt, 1991*a*). On the other hand, the gating of the outward K^+ channel is sensitive to external K^+, activating at voltages consistently positive of the K^+ equilibrium potential (E_{K^+}), for example around -40 mV in 10 mM KCl (Blatt, 1988; Schroeder, 1988). The gating of the outward-rectifying channel, however, appears to be independent of cytoplasmic Ca^{2+} (Schroeder & Hagiwara, 1989).

Such voltage-dependent gating characteristics suggest that variations of the membrane voltage may play, along with modulations of the cytoplasmic Ca^{2+} activity, a key role in the control of channel activity during stomatal movement. If voltage control of K^+ channels was relevant it would imply that additional transport steps are required to activate inward- and outward-rectifying K^+ channels as pathways for K^+ influx and efflux, respectively, for initiation of stomatal movement. Thus for the outward rectifier to function as a pathway for K^+ efflux during stomatal closure, the membrane voltage has to be positive of the activation voltage for the outward rectifier and of the potassium equilibrium potential. In cells with very negative membrane voltages this would require membrane depolarization. In contrast, to allow K^+ influx through the inward-rectifying K^+ channel, with an activation threshold at more negative voltages, the membrane voltage has to be driven negative of -100 mV, possibly by the activity of a H^+ pump (Blatt, 1987*b*) and also, to guarantee passive K^+ influx, negative of E_{K^+}.

Information on the regulation of K^+ fluxes in guard cells during the process of stomatal closure has been obtained with abscisic acid (ABA). This phytohormone is produced in leaves under water stress conditions and is responsible for subsequent stomatal closure, a process consequent on the loss of potassium salts from the stomatal guard cells (MacRobbie, 1981). The mechanism by which the externally acting ABA (Hartung, 1983) promotes salt loss was investigated in intact guard cells under voltage clamp (Blatt 1990), revealing actions of the phytohormone on at least three distinct transport processes. (i) ABA increased the capacity of the outward K^+ channels to pass current but without an effect on the kinetics or voltage dependency for activation and deactivation. (ii) There were indications of a reduction in an inward current at more negative voltages, now recognized to be carried by inward-rectifying K^+ channels (Blatt et al., 1990; Blatt, 1991*a*). (iii) Finally, ABA increased the leak conductance, such that charge balance was maintained by the K^+ outward-rectifier and leak currents with little change in the prevailing membrane voltage.

Some, but not all, of the fluxes and currents can be explained as the consequence of increases in cytoplasmic Ca^{2+} activity as an early event following the ABA stimulus (McAinsh, Brownlee & Hetherington, 1990; Schroeder & Hagiwara, 1990*a*). Elevating cytoplasmic Ca^{2+} activities either through the patch pipette (Schroeder & Hargiwara, 1989) or indirectly by increasing the level of the Ca^{2+} mobilizing second messenger $InsP_3$ (Gilroy, Reed & Trewavas, 1990) was shown to reduce current through the K^+ inward-rectifier, by shifting activation negative-going along the voltage axis, and to activate an inward (anion?) current; but Ca^{2+} does not affect the outward-rectifying K^+ channel (Schroeder & Hagiwara, 1989; Blatt et al., 1990).

In spite of this indirect evidence, the time course(s) and extent to which ABA affects the Ca^{2+} status of guard cells is still being argued in light of conflicting evidence from several laboratories. McAinsh et al. (1990) observed that ABA-evoked stomatal closure was preceded by an increase in cytoplasmic Ca^{2+} activity. The Ca^{2+} signal showed a time course comparable to the second delayed component of the efflux transient (MacRobbie, 1990) and activation of the outward-rectifying K^+ channel (Blatt, 1990). By contrast, Gilroy et al (1991; *see also* Fricker et al., 1991) found an increase in cytoplasmic Ca^{2+} in response to ABA only in a minority of cells, although stomata closed in all cases.

Much of this conflict may relate to questions of the prevailing driving forces and kinetic controls on ion flux across the plasma membrane, both for Ca^{2+} and K^+ (Blatt, 1991*a*). Here it must be stressed that the earlier studies with intact guard cells (Blatt, 1990) showed little primary pump activity. Even before adding ABA, membrane voltages were situated positive of E_{K^+}. Thus, membrane depolarization was not required to activate the K^+ outward-rectifier (Blatt 1990, 1991*a*).

By contrast, this mechanism would not be sufficient to promote K^+ loss from guard cells for which the membrane voltage is well negative of E_{K^+} and

the activation voltage of the outward K^+ current. In the present study we characterize the current-voltage relation of cells which exhibit a considerable primary pump activity. In these cells free-running voltages were often well negative of E_{K^+} and beyond the voltage range activating the K^+ outward-rectifier; rather, the thermodynamic driving force on potassium was heavily biased towards K^+ influx. We show here that, for cells exhibiting membrane voltages substantially negative of E_{K^+}, membrane depolarization is an early and important step leading to net K^+ efflux in ABA. Furthermore, the underlying changes in specific transport currents imply that events leading to the membrane depolarization are allied to a rise in the cytoplasmic Ca^{2+} activity.

Materials and Methods

Plant Material and Experimental Protocol

Vicia faba L. cv (Bunyan) Bunyan Exhibition was grown on vermiculite under conditions described previously (Blatt, 1987*a*,*b*). Epidermal strips were prepared from newly expanding leaves of young (4–5 week) plants. For electrical measurements, strips were affixed to the bottom of the incubation chamber by appressing on to a pressure-sensitive adhesive (No. 355 Medical Adhesive, Dow Corning, Brussels), and all operations were carried out on a Zeiss IM inverted microscope (Zeiss, Oberkochen, FRG) fitted with Nomarski Differential Interference Contrast optics. Measurements were performed in rapidly flowing solution (approx. 20 chamber volumes per min) containing 5 mM MES (2-(N-morpholino)propanesulfonic acid), titrated with $Ca(OH)_2$ to pH 6.1 (final $[Ca^{2+}] \approx 1$ mM) with KCl added as required. Ambient temperatures were 20–25°C.

Stomatal apertures were measured with a calibrated eyepiece micrometer, and guard cell surface areas were calculated from the orthogonal dimensions of the cells, assuming a cylindrical geometry. In the present experiments cell diameters varied between 10 and 15 μm and the cell length between 35 and 40 μm.

Electrical

Mechanical, electrical and software design have been described in detail (Blatt, 1987*a*,*b*, 1990). Recordings were obtained using double-barrelled microelectrodes (Blatt, 1987*a*, 1991*b*). The electrodes were filled with 200 mM K^+-acetate, pH 7.3, to minimize salt leakage and salt-loading artifacts (Blatt, 1987*a*), and were coated with paraffin to reduce electrode capacitance. Current-voltage relations were determined by the two-electrode method with the voltage-clamp circuit under microprocessor control. Steady-state *I-V* relations were recorded by clamping cells to a bipolar staircase of command voltages (Blatt, 1987*b*). Steps alternated positive and negative from V_M (typically 20 bipolar pulse pairs) and were separated by equivalent periods when the membrane was clamped to V_M. The current signal was low-pass filtered by a 6-pole Butterworth filter at 1 or 3 kHz (−3 dB) before sampling, and currents and voltages were recorded during the final 10 msec of each pulse.

For time-dependent characteristics, current and voltage were sampled continuously at 1, 2 or 10 kHz while the clamped voltage was driven through cycles of 1–4, programmable pulse steps. Recordings at 10 kHz (above the Nyquist limit) were restricted by available data storage space to 200-msec "windows" within each cycle; otherwise, data taken at all frequencies gave similar results. In some experiments, current kinetics were recorded using a single set of voltage steps repeated in an open loop (open-loop protocol). In these cases, currents and voltages were digitized at 22 kHz using pulse-code modulation (Sony PCM-701ES, Japan) and stored on video tape for later analysis. No attempt was made to compensate for the series resistance (R_s) to ground (Hodgkin, Huxley & Katz, 1952). Estimates for R_s indicated that it was unlikely to pose a serious problem in measurements of clamp voltage (Blatt, 1988).

Numerical Analysis

Data analysis was carried out using a nonlinear, least-squares algorithm (Marquardt, 1963). The fitting of the recorded membrane voltages to different normal distributions was done by the MLP program package (Ross, 1987). Throughout the paper results are quoted as mean ± SEM of (n) observations.

Chemicals and Solutions

Abscisic acid (racemic) and the pH buffer MES were from Sigma Chemical (St. Louis, MO). Otherwise, all chemicals were Analytical Grade from BDH (Poole, Dorset, UK).

Results

For the total of 43 cells investigated between June and September 1990 the membrane voltages in 0.1 mM KCl, 5 mM Ca-HEPES, pH 7.4, varied between a minimum value of −120 mV and a maximum of −283 mV. To determine whether the large variability in membrane voltages reflects the existence of two different membrane transport states, i.e., a pump-dominated and a diffusion-dominated state (Blatt, 1988, 1990; Blatt & Clint, 1989), the distribution of the recorded membrane voltages were fitted to a number of models; these were (i) a single normal distribution (as a control), (ii) the sum of two normal distributions with equal variances, and (iii) the sum of two normal distributions with unequal variances, using the MLP statistics package (Ross, 1987). Based on the x^2 values as a test of the goodness of fit, it appeared that the data were best fitted by the sum of two normal distributions with unequal variances (Fig. 1). The cells of the two different membrane voltage categories could also clearly be separated by their characteristic current voltage (*I-V*) and conductance-voltage (*G-V*) relations. Figure 2 illustrates two representative *I-V* curves: one from a high voltage cell ($V_M = -191$ mV) and one from a low voltage cell ($V_M = -123$ mV). The *I-V* curve from the high voltage cell exhibits the characteristic

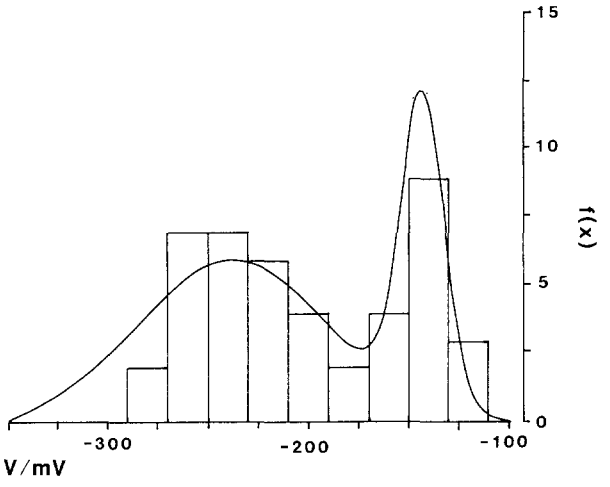

Fig. 1. Sample and fitted frequency distribution of membrane potentials recorded from a total of 43 guard cells, bathed in 0.1 mM KCl, 5 mM Ca^{2+}-HEPES, pH 7.4. The recorded voltages were grouped into categories of 20 mV. The theoretical distributions were fitted to the data using the MLP program package; the best fit was given by two normal distributions with unequal variance, with mean voltages of -143 ± 4 mV and -237 ± 10 mV for the low and high voltage group, respectively.

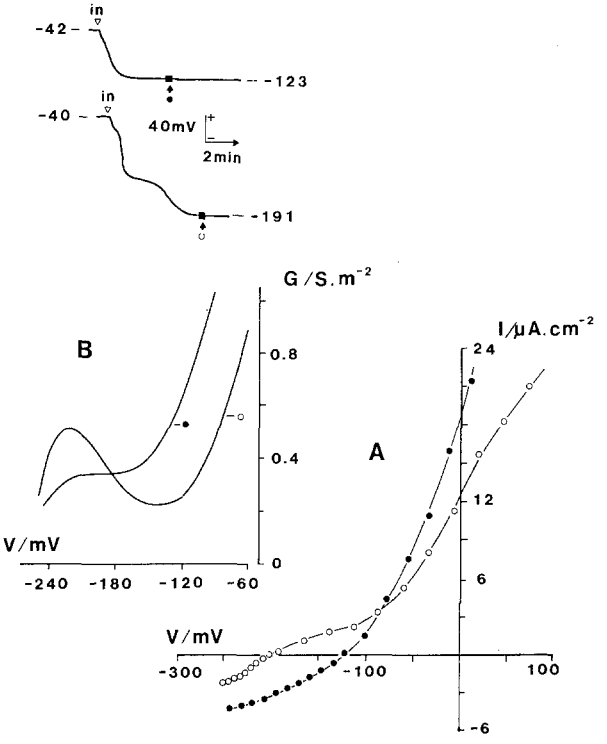

Fig. 2. (*A,B*) Steady-state current-voltage (*I-V*) and conductance-voltage (*G-V*) characteristics for two *Vicia faba* guard cells with different free-running membrane voltages in 0.1 mM KCl, 5 mM Ca^{2+}-HEPES, pH 7.4. *Inset:* After impalement with double-barrelled electrodes for voltage clamping (*in*), one cell (●) reached a low stable membrane voltage of -123 mV, while the other (○) hyperpolarized to a much more negative voltage of -191 mV. (*A*) *I-V* scans were run using a bipolar staircase of voltage commands of 150 msec long pulses (*see* Materials and Methods), during the period masked by bars on the voltage traces. The symbols at the voltage traces cross-reference with the symbols for the *I-V* and *G-V* data. (*B*) Conductance-voltage characteristics for the *I-V* data in *A*, with focus on the voltage range negative of -60 mV. The conductance data were obtained by fitting the *I-V* data in *A* to 8th order polynomials and differentiating. Cell parameters: surface area and stomatal aperture, (●): $1.75 \cdot 10^{-5}$ cm^2, 7.5 μm; (○): $1.9 \cdot 10^{-5}$ cm^2, 8 μm.

pump-related sigmoid curvature at voltages negative of -150 mV, giving a distinct conductance maximum at approximately -230 mV (Blatt, 1987*b*). It was also characteristic of the high voltage cells that the pump conductance appeared on a background of low leak[1] conductance (given approximately by the conductance minimum at -150 mV for cells in 0.1 mM KCl (Blatt, 1987*b*)), so that the ratio of the conductances at -230 mV and at -150 mV, which provides an indirect measure of the pump conductance relative to the leak conductance, was always >1. In contrast, the low voltage cells were characterized by a near linear current for voltages negative of about -150 mV. One characteristic example is shown in Fig. 2; a small conductance maximum near -230 mV was eclipsed by a background of high leak conductance. As a consequence the small pump current contributed relatively little to the charge balance at the resting voltage. It was characteristic of the low voltage cells that the ratio of the conductance at -220 mV to that at -150 mV was <1.

Membrane Voltage and K^+ Transport

The membrane voltage is determining for passive K^+ transport in two respects: The direction for passive K^+ fluxes is set by the situation of V_M in respect to E_{K^+}. On the other hand, the complex voltage-dependent gating of the inward- and outward-rectifying K^+ channels requires an appropriate voltage in the active range of these channels to guarantee the presence of an active transport pathway. To illuminate the relevance of the observed different membrane voltages for the control of K^+ transport, individual cells were assayed for the K^+ equilibrium potential in relation to V_M. Furthermore, *I-V* relations were assayed for the contribution of K^+ currents at the relevant free-running membrane voltage.

The K^+ equilibrium potential was estimated from the reversal voltage for K^+ currents, using the

[1] The term "leak" is used to describe the sum of all as yet unidentified currents.

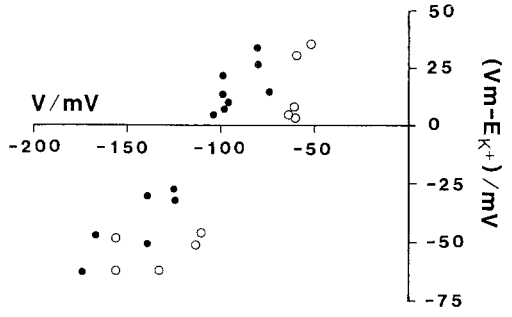

Fig. 3. The deviation of the free-running membrane voltage from the K^+ equilibrium voltage ($V_M - E_{K^+}$) of individual *Vicia* guard cells, in 5 mM Ca^{2+}-MES, pH 6.1, and 3 (●) or 10 (○) mM KCl, as a function of membrane voltage. The K^+ equilibrium voltage was obtained for cells with stable membrane voltages, using the analysis of K^+ tail current relaxation to estimate the K^+ reversal voltage (for further detail *see* Materials and Methods).

analysis of tail currents. This analysis is based on the recording of the relaxation of the K^+ current through the outward rectifier for voltage steps between 0 and −120 mV after an initial activation by a clamp step to +50 mV (Blatt, 1988; for further detail *see* Materials and Methods). Since millimolar concentrations of external K^+ slow down the current relaxation compared to μM concentrations and consequently improve the measurements, cells were transferred into a medium containing 5 mM Ca-MES, pH 6.1, and 3 or 10 mM KCl (the change in pH was designed to allow further investigation of the inward-rectifying K^+ current (*see below*), which is larger at acid pH (Blatt et al., 1990; Blatt, 1991*a*)). Overall, the distinct separation of cells into high and low voltage cells was also maintained in millimolar K^+ concentrations. After transferring cells into test solutions with 3 or 10 mM KCl the cells showed a wide range of stable voltages ranging from −78 to −185 mV in 3 mM K^+ and from −32 to −201 mV in 10 mM K^+.

There was no significant difference between the K^+ equilibrium potentials, and hence cytoplasmic K^+ activities, in the two groups of high voltage and low voltage cells. Overall, in 3 and 10 mM KCl (i.e., K^+ activity 2.76 and 8.9 mM, respectively (Robinson & Stokes, 1959)) the mean reversal potential for K^+ currents was −105 ± 3.3 (14) mV in 3 mM KCl and −73.9 ± 4 (10) mV in 10 mM KCl. This corresponds to a cytoplasmic K^+ activity of 162 ± 16 mM in 3 mM KCl and 159 ± 12 in 10 mM KCl.

Figure 3 shows for cells in 3 and 10 mM K^+, that they could be grouped into two categories, on the basis of the deviation of their membrane voltages from the K^+ equilibrium potential. The low voltage cells exhibited electrical driving forces between 5 and 30 mV for passive K^+ efflux. In contrast, the second group of cells, with more negative membrane voltages, had free-running membrane voltages which were between 56 and 76 mV negative of the estimated K^+ equilibrium potentials, thus providing a considerable driving force for passive K^+ influx.

I-V analysis of the currents at the resting voltage of low voltage cells revealed a scenario comparable to those from previous investigations: V_M was situated positive of the activation voltage for the outward K^+ rectifier so that these cells must have had a bias for net K^+ efflux (*data not shown*; *compare* Blatt, 1988, 1990; Blatt & Clint, 1989).

The K^+ current at the resting voltage of high voltage cells was determined after first clamping guard cells to −120 mV, a voltage at which the K^+ inward rectifier was largely inactivated and this preconditioning voltage was followed by steps to voltages between −150 and −250 mV (Fig. 4). The current response separated into two characteristic components, an instantaneous current and a time-dependent current reflecting the slow activation of the inward rectifier. The data clearly show that, in these high voltage guard cells, the membrane voltage was sufficiently negative to provide a pathway for K^+ uptake into the guard cell. In the example shown the free-running membrane potential was −191 mV. At this potential a K^+ inward current of 1.5 $\mu A \cdot cm^{-2}$ was obtained. This is a measure for the net K^+ inward current under conditions of a free-running membrane potential. Comparable results were obtained in three other cells using similar clamp protocols, and the estimated K^+ currents varied between 0.45 and 1.7 $\mu A \cdot cm^{-2}$.

Guard Cells Can Alternate Spontaneously between Two Transport States

Once cells had achieved either a depolarized or a hyperpolarized membrane voltage in 3 or 10 mM K^+, the recorded voltage remained stable, to within a few mV, for long periods of time (>30 min), unless terminated by experimental treatments or by loss of impalements. However, an interesting observation was the occurrence of spontaneous and fast voltage transitions between the two states. Figure 5 shows examples of such voltage transitions, from the low voltage to the high voltage state and also in the reverse direction. It is important to note that the voltage changes do not arise from a sealing of the recording electrodes; transitions were observed after considerable times of impalement, and the *I-V* curves at the two voltages are not consistent with a simple rise in a nonspecific conductance (*see below*).

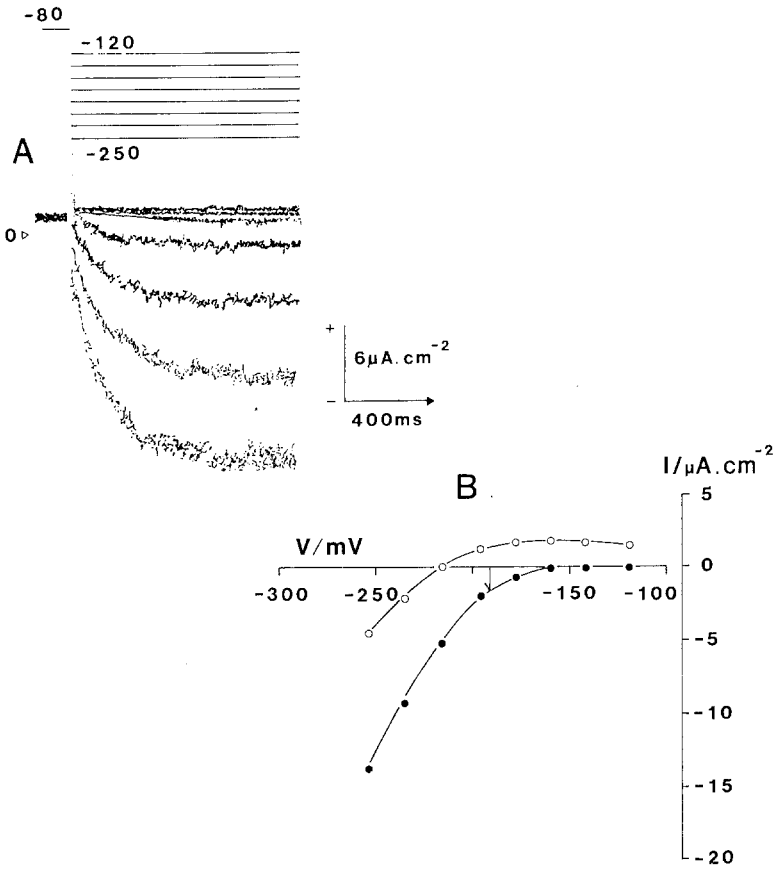

Fig. 4. (*A,B*) Activation of time-dependent currents at negative clamp voltages. The data were collected from one *Vicia faba* guard cell in 5 mM Ca^{2+}-MES, pH 6.1, and 10 mM KCl, with a free-running membrane voltage of −191 mV. (*A*) Currents were recorded from eight clamp cycles between −120 and −250 mV, preceded by preconditioning steps from the resting voltage to −80 mV. (*B*) Dissection of the current responses into the instantaneous current and the slowly activating K^+ channel currents. The fast rising instantaneous currents (○) were taken 4 msec into each test pulse. Subtraction of this current from the steady-state current at the end of each test pulse gave a measure of the slowly activating K^+ current (●). The downward pointing arrow at the resting voltage indicates the magnitude of the K^+ inward current at the free-running voltage. Cell parameters: surface area, $1.6 \cdot 10^{-5}$ cm^{-2}; stomatal aperture, 8 μm.

ABA Promotes Membrane Depolarization in High Voltage Cells

The effect of ABA on the free-running membrane voltage (V_M) depended critically on the underlying background of currents extant prior to the ABA challenge. Abscisic acid evoked appreciable and prolonged membrane depolarizations only in those cells for which V_M was situated negative of E_{K^+} initially. Figure 6 illustrates the effect of ABA on membrane voltages of four *Vicia* guard cells. The cells were bathed in 5 mM Ca^{2+}-MES, pH 6.1, and 3 mM KCl and exhibited a range of membrane voltages between −103 and −144 mV. In three cells the membrane voltage was well negative of the respective equilibrium voltage for K^+ (E_{K^+}) determined from tail current analyses of the K^+ outward rectifier (Blatt, 1988); ABA additions, in each of these cases, evoked large (>40 mV) depolarizations after which V_M lay positive of E_{K^+}. Action potential-like oscillations were occasionally observed (Fig. 6, trace *III*) before the voltage finally settled (4 out of 14 cells). By contrast, the free-running voltage of the fourth guard cell was situated positive of E_{K^+} before ABA addition; in this case, perfusion with 10 μM ABA evoked a much smaller (approx. +10 mV) voltage transient, after which the membrane voltage recovered. In all cases, the final free-running voltage in ABA was situated positive of E_{K^+}.

Membrane depolarizations were observed in 14 other guard cells following the addition of ABA, yielding a mean peak depolarized voltage of −92 ± 8 mV for 7 cells in 3 mM KCl and −33 ± 2 mV for 11 cells in 10 mM KCl. Considering the estimated values for E_{K^+} in 3 and 10 mM KCl (*see above*), membrane voltages in the presence of ABA were observed both on an individual and statistical basis to lie significantly positive of E_{K^+}, at least in 10 mM K^+.

A lag time was characteristic of the response to ABA[2] and, in all but two cells, membrane depolarizations followed within 4 min of adding ABA (mean lag time 83 ± 13 sec; range 10 to 206 sec). The two remaining cells were characterized by extended

[2] Solution exchange and ABA entry into the chamber was timed using the onset of a depolarization evoked by an increase in K^+ concentration as a measure. This lag time for solution entry into the chamber has been taken into account so that time delays reflect the physiological response time in the presence of ABA.

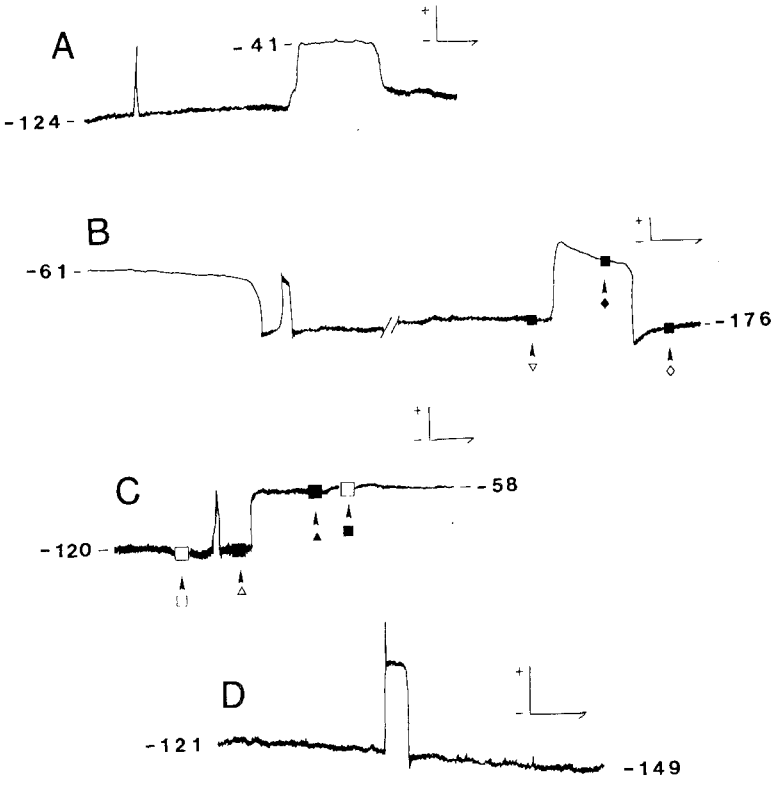

Fig. 5. Spontaneous voltage transitions between low and high voltage states in *Vicia faba* guard cells. Cells were bathed in solutions containing 10 mM KCl and 5 mM Ca^{2+}-MES, pH 6.1. All cells had maintained a constant low voltage (traces *B*) or high voltage (traces *A,C* and *D*) for considerable times before exhibiting spontaneous transitions between the two voltage states. During the periods masked by the bars on the voltage traces *I-V* scans (solid bars) and single clamp pulse protocols (open bars) were recorded, and symbols at the voltage traces correspond to the *I-V* data in Fig. 14 *A–C*. Scales: horizontal, 2 min; vertical, 40 mV.

periods of gradual depolarization before the final transition to voltages positive of E_{K^+} at times 8.5 and 13 min into ABA exposure (*see* Fig. 13).

Underlying Mechanism for ABA-Induced Membrane Depolarization

From previous studies (Schroeder & Hagiwara, 1989, 1990*a*; Blatt, 1990, 1991*a*; Blatt et al., 1990), it was anticipated that the ABA-evoked depolarizations should overlay profound alterations in three distinct conductances, namely those of (i) the K^+ inward rectifier, (ii) the K^+ outward rectifier and (iii) an instantaneous current. The latter reflects the sum of additional conductances as yet uncharacterized in the intact cells, but plausibly includes the anion currents known in the guard cell protoplasts (Schroeder & Hagiwara, 1989; Hedrich et al., 1990). All three currents were assayed during ABA treatments, taking advantage of their respective time- and voltage-dependencies to examine each independently.

Current Activation Analysis ± ABA

Figure 7 illustrates the current for negative clamp voltages before and after an ABA-evoked depolarization. The inward current was again obtained from clamp steps between −150 and −250 after a conditioning pulse to −120 mV.

Following membrane depolarization in ABA, current through the K^+ inward rectifier was reduced, at −230 mV by ca. 12% compared to the pretreatment current. Qualitatively similar results were obtained in four other experiments drawing on time-dependent current dissections, and in all 18 guard cells based on steady-state *I-V* analyses (below). On a quantitative basis, considerable variation was observed in K^+ inward-rectifier response, with current at −230 mV reduced from 9 to 74% of the control.

Current through the K^+ outward-rectifier and its response to ABA was determined after clamping guard cells at a preconditioning voltage of −150 mV to deactivate the current (Fig. 8). Activation of the instantaneous current and the outward time-dependent K^+ current was subsequently recorded on stepping the membrane to test voltages between −80 and +50 mV. These, and steady-state *I-V* analyses (below) confirmed that the outward rectifier did not contribute to charge balance in the absence of ABA for free-running membrane voltages negative of E_{K^+}. Outward-rectifier current was invoked only with membrane depolarization into the voltage region in which the channels were operative. Estimates of the current invoked at V_M in ABA were

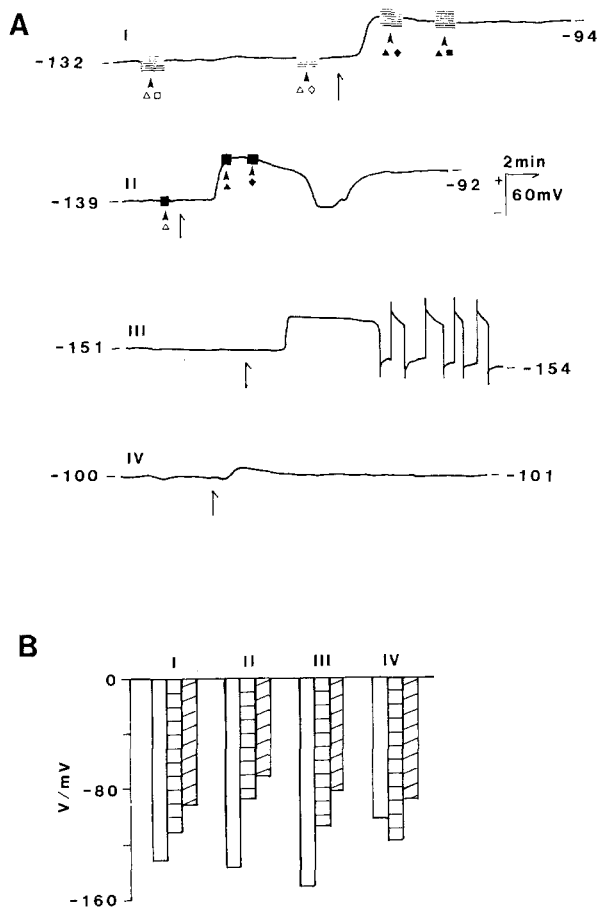

Fig. 6. (*A,B*) Membrane depolarizations in ABA. Data from four *Vicia* guard cells bathed in 5 mM Ca^{2+}-MES, pH 6.1, with 3 mM KCl. (*A*) The voltage response to ABA was first seen following delays of 46 sec (trace *IV*) to 141 sec (trace *III*) after taking into account the time required for ABA to reach the guard cell in each case. The symbols at the voltage traces correspond to symbols of *I-V* plots in Figs. 7–9 (trace *I*) and Fig. 11 (trace *II*). Voltage-clamp data were collected during the periods marked by shading (pulse cycle protocols) or solid bars (bipolar staircase protocols). (*B*) Comparison of the free-running voltage □, the K^+ equilibrium voltage, E_{K^+} ▤, and the peak depolarization voltage ▨ from the four cells in *A* shows membrane voltages in ABA situated positive of E_{K^+}. Values for E_{K^+} were determined from tail current analyses of the K^+ outward rectifier (*see* Blatt, 1988).

obtained from current deactivation on stepping the voltage back to −150 mV from the free-running voltage in ABA. In Fig. 8, the relaxation indicated an outward-rectifier current amplitude of 0.54 $\mu A \cdot cm^{-2}$ for $V_M = -93$ mV after correcting for the difference in driving force ($E_{K^+} = -106$ mV). As in the previous study (Blatt, 1990), ABA treatment also increased the current capacity of the K^+ outward rectifier, for the data in Fig. 8, by a factor of 2.6 following the ABA treatment. Comparable results were obtained in the four other cells examined using these clamp protocols; overall, outward K^+ current was stimulated by factors varying between 1.1 − and 2.73 − fold (mean, 1.73 ± 0.25-fold).

The mechanism underlying the membrane depolarizations was evident on inspecting the background of instantaneous currents. The *I-V* curves in Fig. 9 are composed of these currents pooled between measurements ±ABA from the clamp protocols described above (Figs. 7 and 8). In the absence of ABA the current was outward directed for voltages positive of −180 mV, highlighting primary pump output as a significant component of the current under these conditions. Thus, in the absence of ABA, V_M was determined by a balance between this instantaneous current and the inward-going K^+ current. Since ABA effectively reduced current through the K^+ inward rectifier, the depolarization can only have occurred via a change in the instantaneous current. ABA addition evoked a (downward) shift in the instantaneous current-voltage relation, with the effect that the current was drawn below the voltage axis over the voltage range of membrane depolarization. Again, comparable increases in instantaneous current were recorded following ABA exposures in four other cells examined using theses clamp protocols.

The ABA-evoked changes in instantaneous current are consistent with the activation of a secondary, inward-going current component in the leak. The conclusion is supported by the intersection of the respective *I-V* curves ±ABA at voltages well positive of the proton pump equilibrium potential (Blatt, 1987*b*). A decline in pump output is also conceivable but is not a prerequisite for depolarization. A similar pattern of current responses was observed also in cells with no obvious pump activity.

Figure 10 shows time- and voltage-dependent currents from one *Vicia faba* guard cell with a free-running voltage of −55 mV in 10 mM KCl. In the control, steady-state *I-V* data revealed typical features of the diffusion dominated membrane (*compare* Fig. 10*A* with Blatt et al., 1990). The cell was subjected to an open-loop clamp protocol with voltage steps (700 msec) between the free-running voltage and −150 mV. This operation gave rise to reproducible current activations with the typical instantaneous current and superimposed slow-activating K^+ current. Introducing ABA into the chamber lead to an increase in the instantaneous current and a concomitant decrease in the time-dependent current which, within 1 min of adding ABA, gave evidence of a time-dependent deactivation (Fig. 10*B*). ABA also gave rise to an inward current at the holding voltage of −55 mV (= V_M before ABA addition), resulting in membrane depolarization to −48 mV after the clamp cycle was terminated. Figure 10*C*

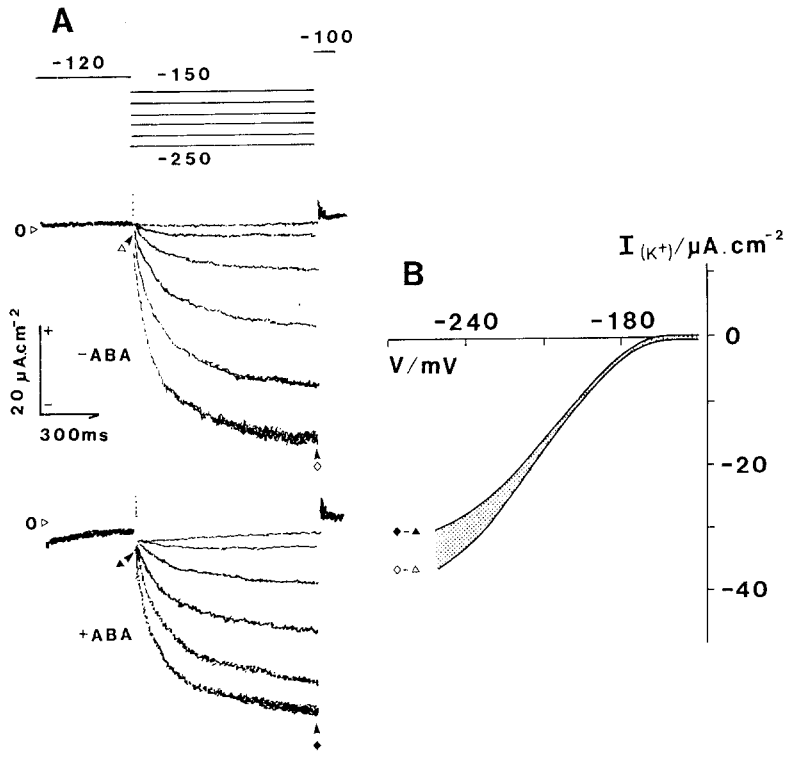

Fig. 7. (*A,B*) K^+ inward-rectifier response to ABA. Data correspond to the clamp cycles immediately before and after ABA addition to the test medium (5 mM Ca^{2+}-MES, pH 6.1, 3 mM KCl) in Fig. 6 (trace *I*, cross-referenced by symbol). Cell parameters: surface area, $1.5 \cdot 10^{-5}$ cm^2; stomatal aperture, 7 μm. (*A*) Currents were activated by a cycle of six clamp steps between −150 and −250 mV following a 700-msec preconditioning step at −120 mV from the free-running voltage (V_M: −ABA, −129 mV; +ABA, −93 mV) to deactivate the current. (*B*) Steady-state K^+ current before (◇ − △) and after (◆ − ▲) adding ABA. Currents were determined by subtracting (in *A*) the instantaneous current (triangles) from the quasi-steady-state values (diamonds) at each voltage. Difference fitted empirically to a 5th-order polynomial. The reduction in K^+ inward-rectifier current is marked by the stippling.

shows the current responses at −150 mV (instantaneous) and −55 mV (steady-state, holding voltage) as they developed with time in ABA. The time courses superimpose, again supporting the conclusion that the instantaneous current drives the membrane positive-going in ABA. Comparable observations were obtained in all five experiments using these clamp protocols, with time lags for the instantaneous current response ranging from 12 to 85 sec following ABA additions.

Steady-State Analysis

The majority of steady-state *I-V* data collected from 18 cells before and after addition of ABA revealed shifts in *I-V* relations comparable to those obtained from the time-dependent current recordings. Examples of steady-state *I-V* profiles from two guard cells, one in 3 and one in 10 mM KCl are shown in Figs. 11 and 12, respectively. Again, ABA-induced membrane depolarization was caused by an increase in inward current over the voltage range of depolarization. In both cells it was possible to approximate a near linear leak current by an extrapolation (Blatt, 1990) from data points about E_{K^+}. Separating the currents revealed that ABA treatment was followed by an increase in outward-rectifying K^+ current, an inhibition in inward-rectifying K^+ current and an increase in the leak current (*compare* Figs. 7–9). The Table summarizes the results from similar experiments in 3 and 10 mM KCl.

It should be noted that three cells challenged with ABA failed to show responses in leak current or, alternatively, in K^+ outward-rectifier current; in one cell, the K^+ current declined following ABA exposure (*data not shown*). In the light of the complex *I-V* characteristics for the instantaneous current in millimolar K^+ (Fig. 9), these observations must be viewed with caution. Analyses based on leak extrapolations yield an approximation only to the individual current responses in ABA. Indeed, it was impossible to estimate a linear leak current for data from six other cells in the presence of ABA (*compare* Fig. 10 and *see below*).

Membrane Depolarization is Associated with the Activation of a Voltage-Dependent Current with Negative Slope Conductance

Steady-state *I-V* data highlighted one additional feature of interest, which is illustrated by data from one cell in Fig. 13. In this case, ABA treatment evoked a voltage-dependent current, activating in the range between about −150 and +50 mV. The appearance of this current resulted in a bi-stable current-voltage

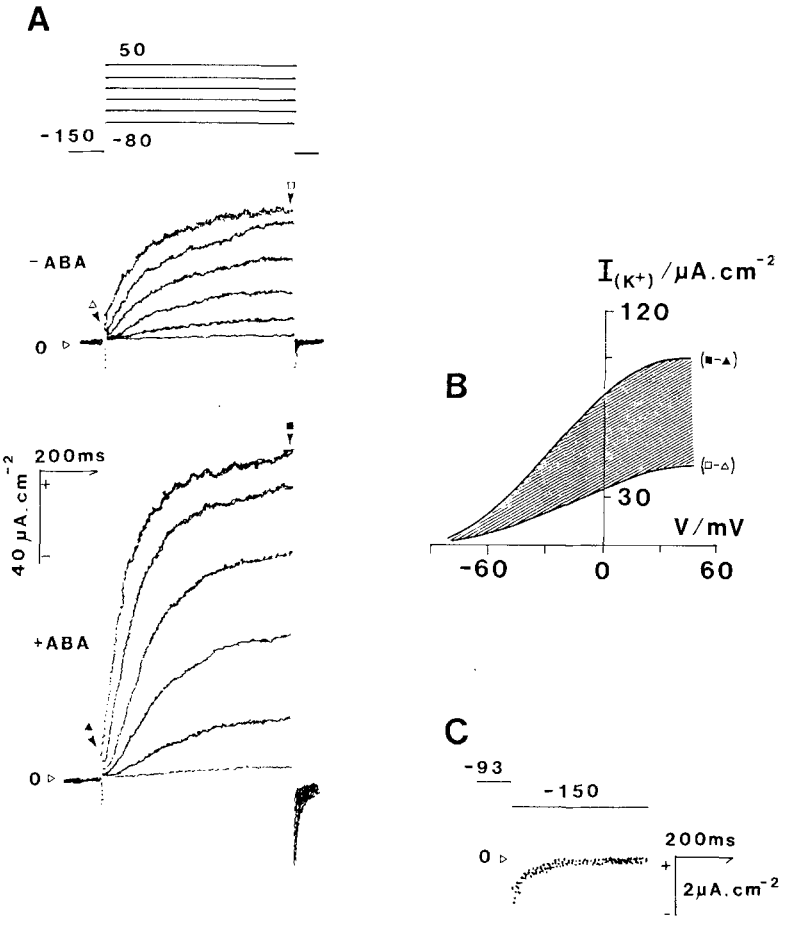

Fig. 8. (*A–C*) K^+ outward-rectifier response to ABA. Data correspond to clamp cycles before and after ABA addition in Fig. 6 (trace *I*, cross-referenced by symbol). Cell parameters are as in Fig. 7. (*A*) Currents were activated by a cycle of six voltage steps between −80 and +50 mV following a 700-msec preconditioning step at −150 mV from the free-running voltage (V_M: −ABA, −131 mV; +ABA, −93 mV) to deactivate the current. (*B*) Steady-state K^+ current before (□ − △) and after (■ − ▲) adding ABA. Currents were determined by subtracting (in *A*) the instantaneous current (triangles) from the quasi-steady-state values (squares) at each voltage. Difference fitted empirically to a 5th-order polynomial. (*C*) Current relaxation on stepping to −150 mV from V_M in ABA. The K^+ outward-rectifier conductance at −93 mV (= V_M) was determined assuming the ohmic relationship, $g_{K^+} = \Delta I/(-150 - E_{K^+})$, from the current relaxation (ΔI) and E_{K^+} (= −106 mV; *see* Fig. 6); g_{K^+} was then applied to determine the corresponding current at V_M, $I_{K^+}[V_m] = g_{K^+}(-93 - E_{K^+})$, yielding a value of 0.5 μA cm^{-2}.

characteristic and negative slope conductance, with the free-running membrane voltage remaining near −150 mV. The current increased in magnitude until the membrane depolarized suddenly to a new stable voltage well positive of E_{K^+}. The current was not observed in all cases with ABA; however, its presence could easily have been masked in steady-state *I-V* profiles, as appears to have occurred in one instance shown in Fig. 11. In this case, the voltage-dependent current was evident only after a decline in K^+ inward-rectifier currents approx. 2 min after adding ABA.

Based on its voltage dependency, this last current activated by ABA appears related to the anion channel already known in the plasma membrane of *Vicia* guard cell protoplasts (Hedrich et al., 1990), although further work will be necessary to establish its identity as such. Were the supposition true, it would account also for the slow deactivating currents which were observed to develop in ABA (*compare* Fig. 10*B* and Hedrich et al., 1990; Schroeder & Hagiwara 1990*b*). [Deactivation here contrasts with that of the K^+ outward rectifier which occurs with halftimes near 15 msec at −150 mV (Blatt, 1988; Schroeder, 1988).]

ABA-Induced and Spontaneously Occurring Voltage Transitions are Correlated with Comparable Effects on Membrane Currents

Steady-state *I-V* scans obtained around spontaneous voltage transition revealed features very similar to those observed after application of ABA. In the cell shown in Fig. 14*A* and *B* the steady-state *I-V* profile and the current response to a hyperpolarizing clamp step were dominated by the typical inward-rectifying K^+ current and the leak current prior to the depolarization. During a spontaneous depolarization the inward-going K^+ current decreased from 5.5 to 3.7 $\mu A \cdot cm^{-2}$. Similar to the situation in the presence of ABA, the instantaneous current increased during depolarization (from 0.2 to 0.8 $\mu A \cdot cm^{-2}$). Comparable observations were made from nine other guard cells.

Figure 14*C* illustrates in an example from one guard cell that in some cases voltage transitions also affected the magnitude of a voltage-dependent current with negative slope conductance. In the present example the peak conductance in the negative slope region increased with the depolarization from −0.075 to −0.12 $S \cdot m^{-2}$, i.e. by 38%. Again, mem-

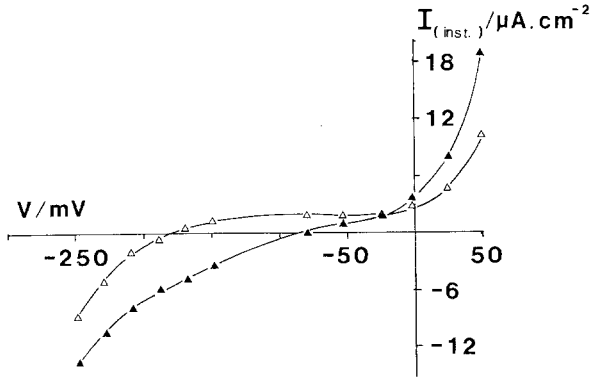

Fig. 9. Instantaneous current response to ABA. Instantaneous currents ($I_{(inst.)}$) from Figs. 7 and 8 before (△) and after (▲) the ABA evoked membrane depolarization. Data were taken 6 msec after the voltage steps to avoid capacitative interference and were fitted to a 6th-order polynomial.

brane depolarization was correlated with a marked decrease in the inward rectifying K^+ current. Similar responses were observed in four other cells showing comparable regions of negative slope conductance.

Discussion

Stomatal Guard Cells under Resting Conditions

The present V_M, *I-V* and *G-V* data confirm and extend previous indications that guard cells exhibit, possibly as seasonal variation, two transport states with very different membrane voltages (Blatt, 1988, 1990; Blatt & Clint, 1989). The interpretation in terms of two states, one dominated by passive diffusion, the other by the activity of the primary pump, is strongly supported by the mathematical model for fitting the present V_M data. Thus the diffusion-dominated cells (low voltage cells) generate membrane voltages over only a small voltage range (small variance), reflecting the fact that only one force is determining the transport properties. The greater variance of the cells in the second, high voltage, group is consistent with the interpretation that in these cells the transport properties are more complex and are dominated by at least two driving forces, namely the electrogenic pump current and the diffusion through the leak. Theoretically the membrane voltage should hyperpolarize to the reversal voltage for the pump, as the contribution of the leak current becomes less important. It is interesting to note that in the fitted distributions the estimated probability becomes very small for voltages more negative than about −350 mV. This is close to the value for the reversal potential of the pump estimated from fittings of pump *I-V* curves (Blatt, 1987*b*), which can be regarded as the theoretical maximum for the membrane voltage.

The difference of pump and leak current contribution to the bulk current in low and high voltage cells is consistent with the respective *I-V* relations of low and high voltage cells (Fig. 1).

K^+ Uptake through Inward-Rectifying Channels

Pump-dominated quard cells were capable of maintaining membrane voltages well negative of E_{K^+} also in millimolar external K^+ concentrations. Separation of currents on the basis of their activation kinetics clearly presents the first direct evidence of current through the inward rectifier at the free-running potential. The estimated net inward current of 1.5 $\mu A \cdot cm^{-2}$ in the cell shown in Fig. 4 is equivalent to a flux of about 16 $pmol \cdot cm^{-2} \cdot sec^{-1}$. The value is very similar to the tracer K^+ influx of 11–16 $pmol \cdot cm^{-2} \cdot sec^{-1}$ measured during the initial opening phase in *Vicia faba* guard cells, but much higher than the influx measured in open guard cells once a steady-state of aperture and K^+ content has been achieved (Fischer, 1972; Pallaghy & Fischer, 1974; Brindley, 1990). Thus the results suggest that the K^+ current through the inward-rectifying K^+ channel is physiologically important for stomatal opening in high voltage cells, in millimolar external K^+.

At the resting voltage the inward K^+ current is balanced by an equal and opposite outward current, the instantaneous current, which must under these conditions reflect the pump current. Its fast activation is consistent with measurements of the Na^+/K^+ pump in heart cells, which showed relaxation times faster than 1 msec in response to clamp steps (Bahinski, Nakao & Gadsby, 1988). It is not possible, however, to discriminate between the fast activation of the pump and of any instantaneous leak current, and it is therefore not possible to equate the total instantaneous current with the pump output.

Modification of Currents in the Dynamics of Stomatal Closure

One way to investigate the signal transduction cascade and the dynamics of stomatal movement is to perturb the steady-state condition by a known stimulus-inducing movement. The effect of the stimulus must then be traced back to the processes controlling the underlying ion fluxes. In the case of

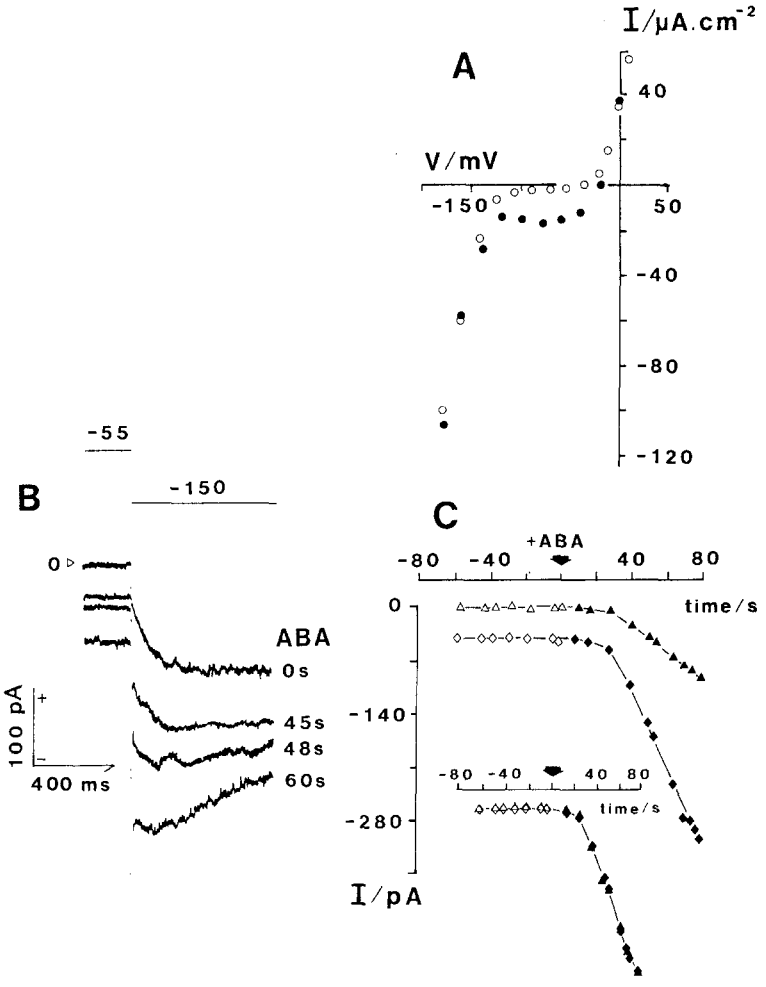

Fig. 10. (*A–C*) Effect of ABA on the leak in the absence of significant pump activity. Data from one *Vicia* guard cell bathed in 5 mM Ca^{2+}-MES, pH 6.1, with 10 mM KCl. Cell parameters: surface area, $1.5 \cdot 10^{-5}$ cm^2; stomatal aperture, 8.5 μm. (*A*) Steady-state *I-V* curves obtained using the bipolar staircase protocol. Scans run before (○) and 180 sec after (●) adding 10 μM ABA to the chamber. Note the region of apparent negative slope (conductance) about −100 mV in ABA. (*B*) Time-dependent current response to ABA, comprising the K^+ inward rectifier and leak currents. The cell was subjected to a continuous loop of 700-msec clamp steps from the holding voltage [= V_M(−ABA) = −55 mV] to −150 mV. Current relaxations at four time points highlight the rise in instantaneous leak current, including the appearance (60 sec time point) of a slow deactivating component. (*C*) Time course for the ABA-evoked rise in instantaneous current (−ABA◇; +ABA◆) sampled 6 msec after clamp steps) and steady-state current at the holding voltage (−ABA△; +ABA▲). *Inset:* Time courses replotted after scaling to a common ordinate.

ABA, a signal-inducing net loss of K^+ salts and consequent stomatal closing (MacRobbie, 1981), one aspect of flux control, was apparent in an ABA-dependent rise in the capacity of the K^+ outward rectifier. In this respect the results outlined above (Figs. 8, 11 and 12) corroborate a previous observation with intact *Vicia faba* guard cells (Blatt, 1990). The present data illustrate another important aspect of flux control, namely the role of membrane depolarization in ABA. Significantly, the prominence of the voltage transition is linked to the transport history of the guard cells prior to ABA treatment. In guard cells for which membrane voltages were situated positive of E_{K^+} (Blatt, 1990), ABA needed only to enhance the existing bias for K^+ loss by increasing the conductance of the K^+ outward rectifier and leak. By contrast, for situations in which V_M lay well negative of E_{K^+}, depolarization must be considered *essential* for net K^+ efflux from guard cells, and goes hand-in-hand with guard cell capacity to utilize the K^+ inward rectifier as a pathway for K^+ uptake in millimolar external K^+.

ABA and the H^+ Pump

The observed scenario, that the pump current is balanced by a K^+ inward current, shows that the net K^+ influx is a direct function of the pump output. This is similar to the situation suggested by previous patch-clamp experiments in guard cell protoplasts (Schroeder, 1988). There it was argued that agents such as fusicoccin or blue light stimulated the pump, resulting in extracellular acidification, and enhanced an inward current, probably a K^+ current.

Also arguments surrounding the mechanism of K^+ efflux in general and in particular ABA-evoked loss of K^+ salts have often focused on H^+ pump activity. It was found early on that ABA treatments resulted in extracellular alkalinizations or, at least, rapid declines in transport-related acidification of

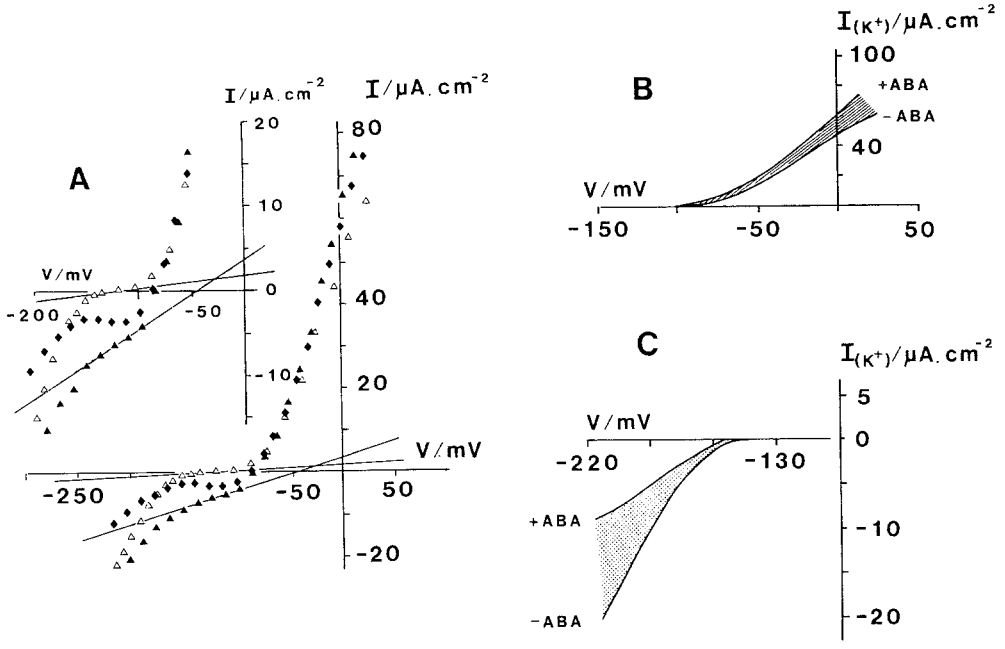

Fig. 11. (*A–C*) Steady-state current response to ABA in 3 mM KCl. Data from one *Vicia* guard cell bathed in 5 mM Ca^{2+}-MES, pH 6.1, and 3 mM KCl. Cell parameters: surface area, $1.9 \cdot 10^{-5}$ cm^2; stomatal aperture, 9 μm. (*A*) *I-V* scans (bipolar staircase protocol, 500-msec pulse lengths) were run shortly before (△) and after (▲, ◆) adding ABA to the bath. Symbols cross-referenced to the time *I-V* scans were run in the corresponding voltage trace (Fig. 6, trace *II*). Before and shortly after adding ABA it was possible to approximate a linear leak current (lines) by extrapolation through data points about E_{K^+}. *Inset:* Linear regions detailed in exploded view. Intersection of the leak lines suggests a reversal voltage at −26 mV. (*B*) K^+ outward-rectifier current estimated by subtracting the extrapolated leak current positive of E_{K^+}. Shading indicates the extent of ABA-induced enhancement. Curves fitted to 5th-order polynomials. (*C*) K^+ inward-rectifier current estimated by subtracting the extrapolated leak current negative of E_{K^+}. Stippling indicates the extent of ABA dependent inactivation. Curves fitted to 5th-order polynomials.

the medium around a variety of plant tissues (Rayle, 1973; Lado, Rasi-Caldogno & Colombo, 1975; but *see also* Gepstein, Jacobs & Taiz, 1982); the suggestion was that an inhibition of the H^+ pump and a consequent depolarization (Kasamo, 1981) was an early event in the mode of ABA action. The present data do not rule out an ABA sensitivity of pump output. Nonetheless, voltage-clamp analyses clearly demonstrate that the scenario of current alterations in ABA—and K^+ efflux enhancement—can occur independent of detectable pump activity (Fig. 10, *see also* Blatt, 1990).

Nature of the Leak Conductance

Abscisic acid was observed to activate a voltage-dependent current (Figs. 10 and 13) with characteristics analogous to a Ca^{2+}- and nucleotide-sensitive anion channel known in *Vicia* guard cell protoplasts (Hedrich et al., 1990). This current probably contributes to charge balance and net solute efflux in ABA (*see* Fig. 13), but it is a poor candidate as the initial trigger for membrane depolarizations. Its fixed voltage dependence for gating limits the voltage span over which it can effect depolarization to voltages positive of an activation "threshold" near −130 to −150 mV (Figs. 10 and 13); yet, under the same conditions, the guard cells frequently exhibited free-running voltages well negative of this value (for example *see* Fig. 3). More likely, activation of this current is secondary and probably a consequence of a rise in cytoplasmic Ca^{2+} activity (*see below*). This view is consistent also with the slower appearance of a second current deactivating at −150 mV (Fig. 10*B*).

Abscisic acid was observed to promote additional inward-going current(s) with a nearly linear conductance profile (Figs. 9, 11 and 12; *see also* Blatt, 1990), and, in view of its near voltage insensitivity, it is this conductance which must provide the prime mechanism for depolarizations. Details of the ionic nature of this current remains unknown. However, there are some indications that a significant component of this current may be carried by K^+, but via a pathway distinct from either of the dominant K^+ channels already identified at the guard cell plasma membrane. Extrapolating leak currents,

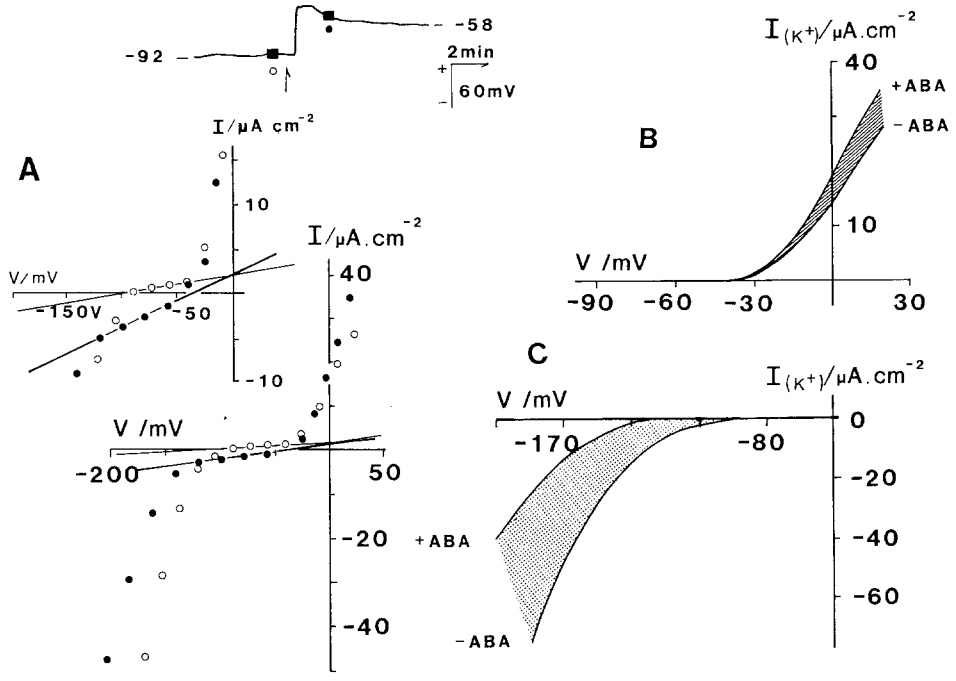

Fig. 12. (*A–C*) Steady-state current response to ABA in 10 mM KCl. Data from one *Vicia* guard cell bathed in 5 mM Ca^{2+}-MES, pH 6.1, and 10 mM KCl. Cell parameters: surface area, $1.8 \cdot 10^{-5}$ cm^2; stomatal aperture, 7 μm. (*A*) *I-V* scans (bipolar staircase protocol, 700-msec pulse lengths) were run shortly before (○) and after (●) adding ABA to the bath. Symbols cross-referenced to the time *I-V* scans were run in the corresponding voltage trace (*Inset, above:* ↑, ABA entry into the chamber). Before, and after adding ABA it was possible to approximate a linear leak current (lines) by extrapolation through data points about E_{K^+}. *Inset, below:* Linear regions detailed in exploded view. Intersection of the leak lines suggests a reversal voltage at +2 mV. (*B*) K^+ outward-rectifier current estimated by subtracting the extrapolated leak current positive of E_{K^+}. Shading indicates the extent of ABA-induced enhancement. Curves fitted to 5th-order polynomials. (*C*) K^+ inward-rectifier current estimated by subtracting the extrapolated leak current negative of E_{K^+}. Stippling indicates the extent of ABA-dependent inactivation. Curves fitted to 5th-order polynomials.

Table. Effect of ABA on the slope conductance of the fitted near-linear leak current and on the current carried by the inward- and outward-rectifying K^+ channels at −200 mV (inward K^- current) and 0 mV (outward K^+ current)[a]

$[K^+]_o$/mM	3	10
G (leak)	+73 ± 20 (5) [29–157]	+69 ± 40 (4) [15–168]
$I_{K^+,in}$ (−200 mV)	−36 ± 12 (5) [11– 85]	−28 ± 18 (4) [12– 53]
$I_{K^+,out}$ (0 mV)	+33 ± 7 (5) [13– 54]	+28 ± 10 (4) [14– 56]

[a] The data were obtained from steady-state *I-V* plots recorded before and >5 min after adding ABA to the bath. The K^+ current component was estimated by subtracting an approximated leak current obtained from linear extrapolation of a linear region of the *I-V* curve (*compare* Figs. 11 and 12). Data are presented as the percentage of changes in current and conductance values following addition of ABA. Values in parentheses are number of cells, and values in square brackets are minimum–maximum of all observations.

ABA yielded apparent reversal voltages which were displaced systematically positive-going in 10 mM KCl compared to 3 mM KCl (*compare* Figs. 9, 11 and 12); in a total of eight cells, mean apparent reversal voltages were −26 ± 4 and −4 ± 8 in 3 and 10 mM KCl, respectively, and differed significantly at the 5% level (*t*-test). Comparable results were obtained also for the reversal voltage of instantaneous currents ABA (e.g. Fig. 9) giving apparent reversal voltages of −24 ± 3 mV (n = 5) in 3 mM KCl for two cells in 10 mM KCl, −4 and −12 mV.

The possibility of an additional pathway for K^+ efflux allies the present electrical data with recent tracer flux measurements in isolated *Commelina*

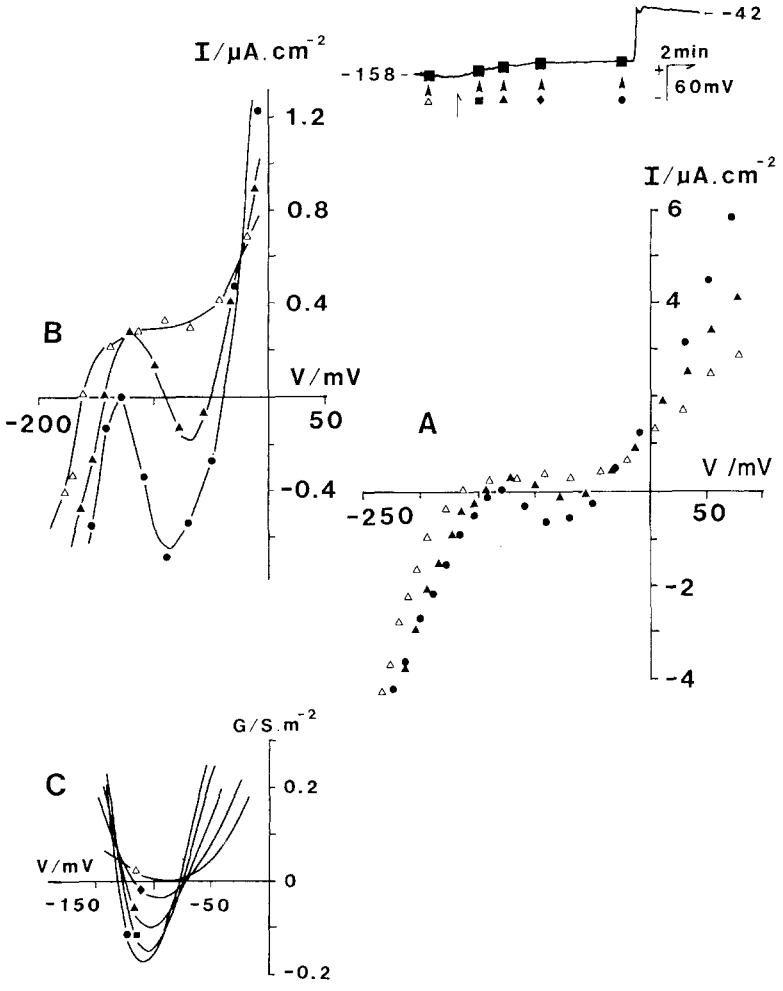

Fig. 13. (*A–C*) Appearance of voltage-dependent current in the presence of ABA. Data from one *Vicia* guard cell bathed in 5 mM Ca^{2+}-MES, pH 6.1, with 10 mM KCl. Cell parameters: surface area, $1.3 \cdot 10^{-5}$ cm^2; stomatal aperture, 9.5 μm. (*A*) *I-V* data from a bipolar staircase protocol of 700-msec pulse lengths before adding ABA (△) and after it entered the chamber (▲, ●). For clarity only selected *I-V* scans are shown. *Inset:* corresponding voltage trace indicating the periods of *I-V* scans (solid bars, cross-referenced by symbol to the *I-V* data in *A–C*) and the time of ABA entry into the chamber (↑). (*B*) Exploded view of the currents near −100 mV in *A*. (*C*) Slope conductances obtained by differentiating 8th-order polynomial fittings of all of the *I-V* data.

guard cells. MacRobbie (1990) found that ABA exposures yielded two distinct phases to the time course for K^+($^{86}Rb^+$) efflux. A slow rise in efflux rate occurred over 2–10 min, and compares favorably with the time course for activation of the outward-rectifying K^+ channels (Blatt, 1990). In addition, an initial phase to the efflux was characterized by a transient rise in flux rate which peaked within 30 sec. Leak activation (Fig. 10) shows a time course comparable to that of this first efflux transient, suggesting its possible contribution to this rapid flux transient.

It must be noted that this apparent reversal voltage was always found to lie positive of E_{K^+} (Figs. 11 and 12) and ABA consistently drove V_M positive of E_{K^+}. Both observations point to another ion (or ions) contributing to this current. Schroeder and Hagiwara (1990*a*) have proposed the operation of a non-selective and Ca^{2+}-permeable channel to account for voltage-dependent increases in the cytoplasmic Ca^{2+} activity of guard cell protoplasts in response to ABA.

Finally it must be stressed that the complex nature of the leak current, i.e., the nonlinear current-voltage relation, the apparent ion selectivity and the sensitivity to ABA strongly argue for a physiological relevance of this current or currents. These features, in particular the ABA sensitivity, would not be expected if the current was an electrode leak conductance produced by impalement.

Ca^{2+} and Transport Control

A similar mechanism in which a Ca^{2+} flux contributes to the leak current evoked by ABA would also explain the present findings. Assuming a cytoplasmic activity around 1 μM in ABA, $E_{Ca^{2+}}$ would be near +80 mV across the plasma membrane with 1 mM Ca^{2+} in the bath; so, the thermodynamic driving force would be for Ca^{2+} influx across the entire physiological voltage range, and could account for the leak reversal voltage situated positive of E_{K^+}. There is additional evidence, with ABA treatments,

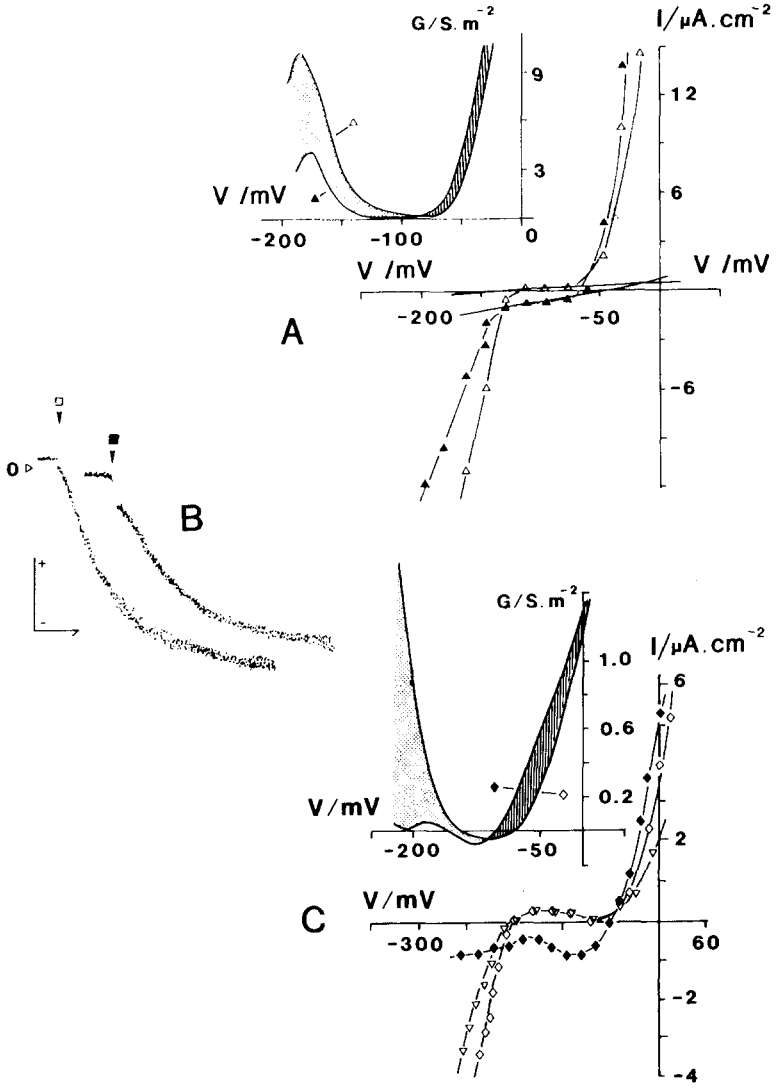

Fig. 14. (*A–C*) Changes in the steady-state *I-V* and *G-V* characteristics associated with spontaneous depolarizations. Two *Vicia faba* guard cells bathed in 10 mM KCl, 5 mM Ca^{2+}-MES, pH 6.1. (Cell parameters: surface area and stomatal aperture, *A*: $2.05 \cdot 10^{-5}$ cm^2, 6.5 μm, *C*: $1.95 \cdot 10^{-5}$ cm^2, 9 μm) were subjected to *I-V* scans with bipolar staircase clamp protocols (700 msec long pulses) in the hyperpolarized state (open symbols) and at depolarized voltages (filled symbols). Corresponding voltage traces in Fig. 5 indicate the period of data collection. In *A* it was possible to approximate a linear leak current (lines) by extrapolation through data points about E_K before and after depolarization. *Insets:* Slope conductance voltage curves corresponding to the *I-V* data from depolarized and hyperpolarized states. *G-V* curves were obtained by differentiating 6th order polynomials fitted to the *I-V* data. The conductance enhanced in the process of depolarization is indicated by shading, while the inhibited conductance is illustrated by stippling. (*B*) Time-dependent current response before (□) and after (■) depolarization comprising the K^+ inward-rectifier and instantaneous leak currents. The cell (same as in *A*, periods of data collection indicated in Fig. 5) was subjected to an open loop clamp protocol of 1000-msec clamp steps between −80 and −180 mV. The arrowheads indicate the clamp step from −80 to −180 mV (filled arrowhead) and the 0 current level (open arrowhead). Sampling frequency, 2 kHz. Scales: horizontal, 200 msec; vertical, 2 $\mu A \cdot cm^{-2}$.

for a rise in cytoplasmic Ca^{2+} activity which would be expected to follow transmembrane Ca^{2+} influx (Schroeder & Hagiwara, 1990*b*): a direct parallel can be drawn to the K^+ inward-rectifier response (Figs. 7 and 10–12) and its inactivation observed on loading guard cell protoplasts with Ca^{2+} from a patch pipette (Schroeder & Hagiwara 1990*a*) or after mobilizing intracellular Ca^{2+} via the second messenger inositol 1,4,5-tris-phosphate (Blatt et al., 1990; Gilroy et al., 1990). The cytoplasmic Ca^{2+} signal would also account for the inward-going current evoked between −50 and −150 mV, assuming that this reflects an activation of Ca^{2+} sensitive anion channels (Hedrich et al., 1990). Such emphasis of thinking on transmembrane Ca^{2+} flux complements earlier work on an apparent requirement in stomatal closure for extracellular Ca^{2+} (De Silva, Hetherington & Mansfield, 1985).

Most interestingly the same, apparently Ca^{2+} sensitive currents affected by ABA were also altered in association with spontaneous voltage transitions. Thus, changes in the cytoplasmic Ca^{2+} activity are very likely to play also a key role in the underlying mechanism leading to these spontaneous voltage transitions. Consequently, it is tempting to speculate that membrane depolarizations mediated by cytoplasmic Ca^{2+} are not strictly associated with the action of the ABA agonist but provide the guard cell with a more genuine mechanism for transport control.

Still, any conclusion about the primacy of the Ca^{2+} signal is premature. It is important to note that the near-linear leak current is, itself, Ca^{2+} sensitive, and that membrane depolarization can be induced in intact *Vicia* guard cells by means of $InsP_3$-mediated Ca^{2+} mobilization (Blatt et al., 1990). Furthermore,

the same Ca^{2+}-sensitive leak current also increases during spontaneous occurring depolarizations. This would make ad hoc postulates of agonist (i.e., ABA) activation of the channel protein unnecessary. In the case of abscisic acid action the agonist could generate Ca^{2+} release from internal stores as a first step in an ensuing cascade of Ca^{2+}-dependent currents engendered within the leak. It would be easier to understand the bi-phasic chararacteristic of K^+($^{86}Rb^+$) tracer efflux and its late dependence on extracellular Ca^{2+} (MacRobbie, 1990) in this context as well.

Finally it must be mentioned that there is evidence also for ABA-evoked transport independent of Ca^{2+}-related signalling pathways; notably, current through the K^+ outward rectifier has been found to be insensitive to Ca^{2+} (Schroeder & Hagiwara, 1989) and $InsP_3$ (Blatt et al., 1990), although the current is promoted by ABA. The implication is for a more complex cascade of events in which Ca^{2+} influx across the plasma membrane and a rise in intracellular Ca^{2+} levels are only one part. In fact, measurements of cytoplasmic pH and Ca^{2+} activities with fluorescent dyes have demonstrated a dual effect of ABA in corn and parsley, with increases in Ca^{2+} activity occurring together with cytoplasmic alkalinization (Gehring, Irving & Parish, 1990). Thus, pH_i could provide an important clue to identifying another major branch in ABA signal transduction. New data has indicated a role for cytoplasmic pH (Blatt, 1991*a*) in controlling K^+ channel activities of *Vicia* guard cells, and its link to ABA and other physiologically important stimuli is now being explored.

We thank Dr. C. Gilligan for statistical treatment of the V_M data and Prof. D. Gradmann for his critical comments on the manuscript. This work was possible with the aid of an equipment grant from the Gatsby Foundation. G. Thiel was supported by the Science and Engineering Research Council.

References

Bahinski, A., Nakao, M., Gadsby, D.C. 1988. Potassium translocation by the Na^+/K^+ pump is voltage insensitive. *Proc. Natl. Acad. Sci. USA* **85:**3412–3416

Blatt, M.R. 1987*a*. Electrical characteristics of stomatal guard cells: The ionic basis of the membrane potential and the consequence of potassium chloride leakage from microelectrodes. *Planta* 170:272–287

Blatt, M.R. 1987*b*. Electrical characteristics of stomatal guard cells: The contribution of ATP-dependent, "electrogenic" transport revealed by current-voltage and difference-current-voltage analysis. *J. Membrane Biol.* **98:**257–274

Blatt, M.R. 1988. Potassium-dependent bipolar gating of potassium channels in guard cells. *J. Membrane Biol.* **102:**235–246

Blatt, M.R. 1990. Potassium channel currents in intact stomatal guard cells: Rapid enhancement by abscisic acid. *Planta* **180:**445–455.

Blatt, M.R. 1991*a*. Ion channel gating in plants: Physiological implications and integration for stomatal function. *J. Membrane Biol.* **124:**95–112

Blatt, M.R. 1991*b*. A primer in plant electrophysiological methods. *In:* Methods in Plant Biochemistry. Vol. 6, pp. 281–321. K. Hostettmann, editor Academic, London

Blatt, M.R., Clint, G.M. 1989. Mechanisms of fusicoccin action kinetic modification and inactivation of potassium channels in guard cells. *Planta* **178:**509–523

Blatt, M.R., Thiel, G., Trentham, D.R. 1990. Reversible inactivation of K^+ channels of *Vicia* stomatal guard cells following the photolysis of caged inositol 1,4,5-trisphosphate. *Nature* **346:**766–769

Brindley, H.M., 1990. Fluxes of $^{86}Rb^+$ in "isolated" guard cells of *Vicia faba* L. *Planta* **181:**432–439

Clint, G.M., Blatt, M.R. 1989. Mechanisms of fusicoccin action: Evidence for concerted modulations of secondary K^+ transport in a higher-plant cell. *Planta* **178:**495–508

De Silva, D.L.R., Hetherington, A.M., Mansfield, T.A. 1985. Synergism between calcium ions and abscisic acid in preventing stomatal opening. *New Phytol.* **100:**473–482

Fischer, R.A. 1972. Aspects of potassium accumulation by stomata of *Vicia faba*. *Austr. J. Biol. Sci.* **25:**1107–1123

Fricker, M.D., Gilroy, S., Read, N.D., Trewavas, A.J. 1991. Visualisation and measurement of the calcium message in guard cells. *In:* Molecular Biology of Plant Development. W. Schuch and G. Jenkins, editor. Cambridge University Press, Cambridge

Gehring, C.A., Irving, H.R., Parish, R.W. 1990. Effects of auxin and abscisic acid on cytosolic calcium and pH in plant cells. *Proc. Natl. Acad. Sci. USA* **87:**9645–9649

Gepstein, S., Jacobs, M., Taiz, L. 1982. Inhibition of stomatal opening in *Vicia faba* epidermal tissue by vanadate and abscisic acid. *Plant Sci. Lett.* **28:**63–72

Gilroy, S., Fricker, M.D., Read, N.D., Trewavas, A.J. 1991. Imaging the release of calcium from organelles during stomatal closure. *Plant Cell* **3:**333–344

Gilroy, S., Read, N.D., Trewavas, A.J. 1990. Elevation of cytoplasmic calcium by caged calcium or caged inositol trisphosphate initiates stomatal closure. *Nature* **346:**769–771

Hartung, W. 1983. The site of action of abscisic acid at the guard cell plasmalemma of *Valerianella locusta*. *Plant Cell Environ.* **6:**427–428

Hedrich, R., Busch, H., Raschke, K. 1990. Ca^{2+} and nucleotide dependent regulation of voltage dependent anion channels in the plasma membrane of guard cells. *EMBO J.* **9:**3889–3892

Hodgkin, A.L., Huxley, A.F., Katz, B. 1952. Measurements of current-voltage relations in the membrane of the giant axon of *Loligo*. *J. Physiol.* **116:**424–448

Hosoi, S., Iino, M., Shimazaki, K. 1988. Outward rectifying K^+ channel in stomatal guard cell protoplasts. *Plant Cell Physiol.* **29:**907–911

Kasamo, K. 1981. Effect of abscisic acid on the K^+ efflux and membrane potential of *Nicotiana tabacum* L. leaf cells. *Plant Cell Physiol.* **22:**1257–1267

Keller, B.U., Hedrich, R., Raschke, K. 1989. Voltage-dependent anion channels in the plasma membrane of guard cells. *Nature* **341:**450–453

Lado, P., Rasi-Caldogno, F., Colombo, R. 1975. Acidification of the medium associated with normal and fusicoccin-induced seed germination. *Physiol. Plant.* **34:**359–364

MacRobbie, E.A.C. 1981. Effect of ABA on "isolated" guard cells of *Commelina communis* L. *J. Exptl. Bot.* **32:**563–572

MacRobbie, E.A.C. 1990. Calcium-dependent and calcium-independent events in the initiation of stomatal closure by abscisic acid. *Proc. R. Soc. London B.* **241:**214–219

Marquardt, D. 1963. An algorithm for least-squares estimation of nonlinear parameters. *J. Soc. Ind. Appl. Math.* **11:**431–441

McAinsh, M., Brownlee, C., Hetherington, A. 1990. Abscisic acid-induced elevation of cytosolic free Ca^{2+} precedes stomatal closure. *Nature* **343:**186–188

Pallaghy, C.K., Fischer, R.A. 1974. Metabolic aspects of stomatal opening and ion accumulation by guard cells in *Vicia faba*. *Z. Pflanzenphysiol.* **71:**332–344

Rayle, D.L. 1973. Auxin-induced hydrogen ion secretion in *Avena* coleoptiles and its implications. *Planta* **114:**63–73

Robinson, R., Stokes, R. 1959. Electrolyte solutions, Butterworth, London

Ross, G.J.S. 1987. Maximum Likelihood Program. Numerical Algorithms, Oxford

Schroeder, J.I. 1988. K^+ transport properties of K^+ channels in the plasma membrane of *Vicia faba* guard cells. *J. Gen. Physiol.* **92:**667–683

Schroeder, J.I., Hagiwara, S. 1989. Cytosolic calcium regulates ion channels in the plasma membrane of *Vicia faba* guard cells. *Nature* **338:**427–430

Schroeder, J.I., Hagiwara, S. 1990*a*. Repetitive increases in cytosolic Ca^{2+} of guard cells by abscisic acid: Activation of nonselective Ca^{2+} permeable channels. *Proc. Natl. Acad. Sci. USA* **87:**9305–9309

Schroeder, J.I., Hagiwara, S. 1990*b*. Voltage-dependent activation of Ca^{2+}-regulated anion channels and K^+ uptake channels in *Vicia faba* guard cells. *In:* Calcium and Plant Growth and Development. Vol. 4, pp. 144–150. R.T. Leonard, and P.K. Hepler, Editors. *Am. Soc. Plant Physiol. Symp. Series*, Rockville (MD)

Schroeder, J.I., Raschke, K., Neher, E. 1987. Voltage dependence of K^+ channels in guard-cell protoplasts. *Proc. Natl. Acad. Sci. USA* **84;**4108–4112

Received 1 May 1991; revised 22 October 1991